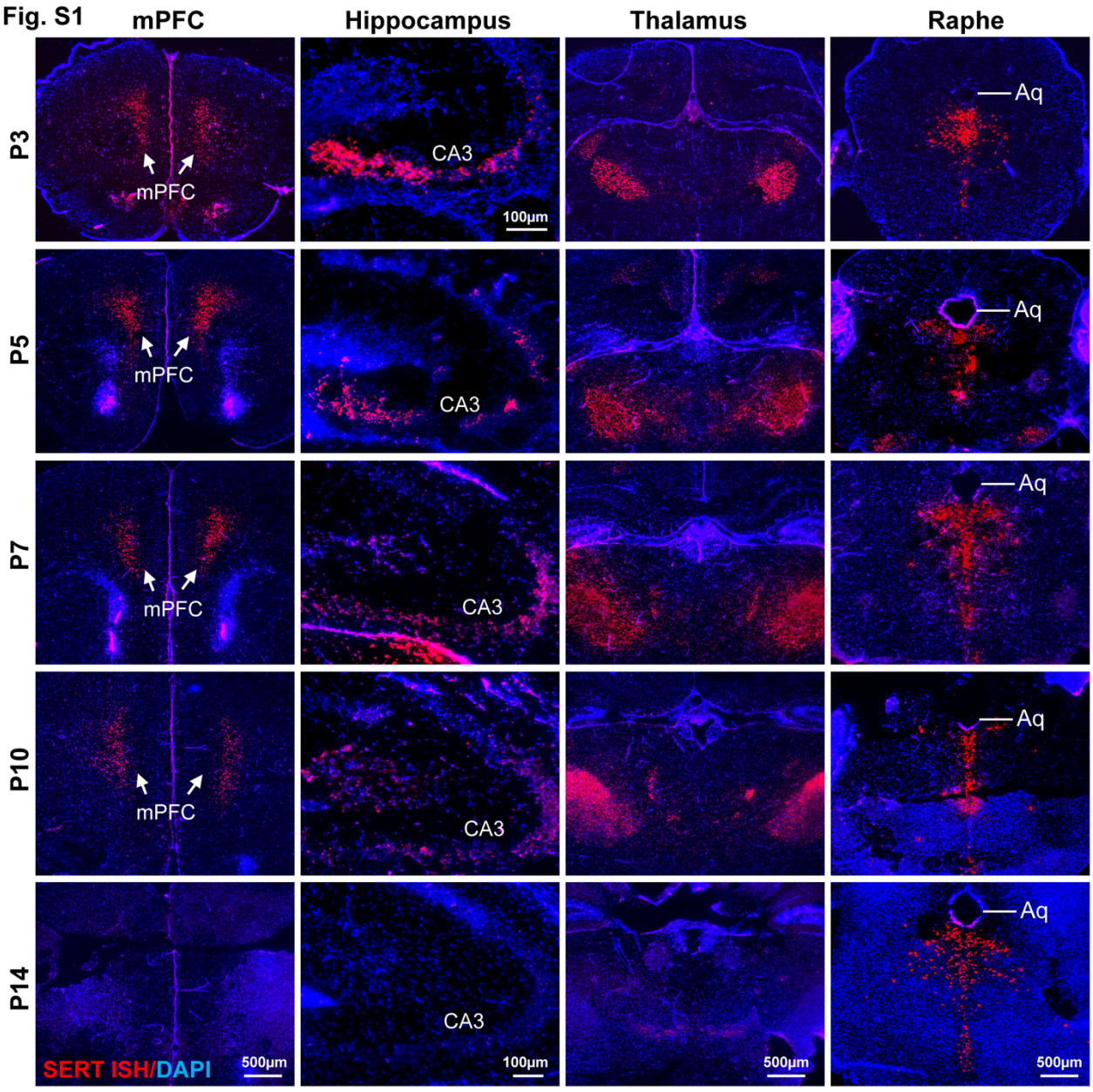

Fig. S1. Time course of SERT expression in glutamatergic neurons. Representative images of SERT mRNA *in situ* hybridization showing temporal-specific transient SERT expression in glutamatergic neurons specifically in the mPFC, hippocampal CA3 and thalamus, contrasting to lifelong continuous SERT expression in raphe serotonergic neurons. Three independent experiments, n = 3 mice/age. mPFC medial prefrontal cortex, Aq aqueduct.

Development • Supplementary information

Fig. S2

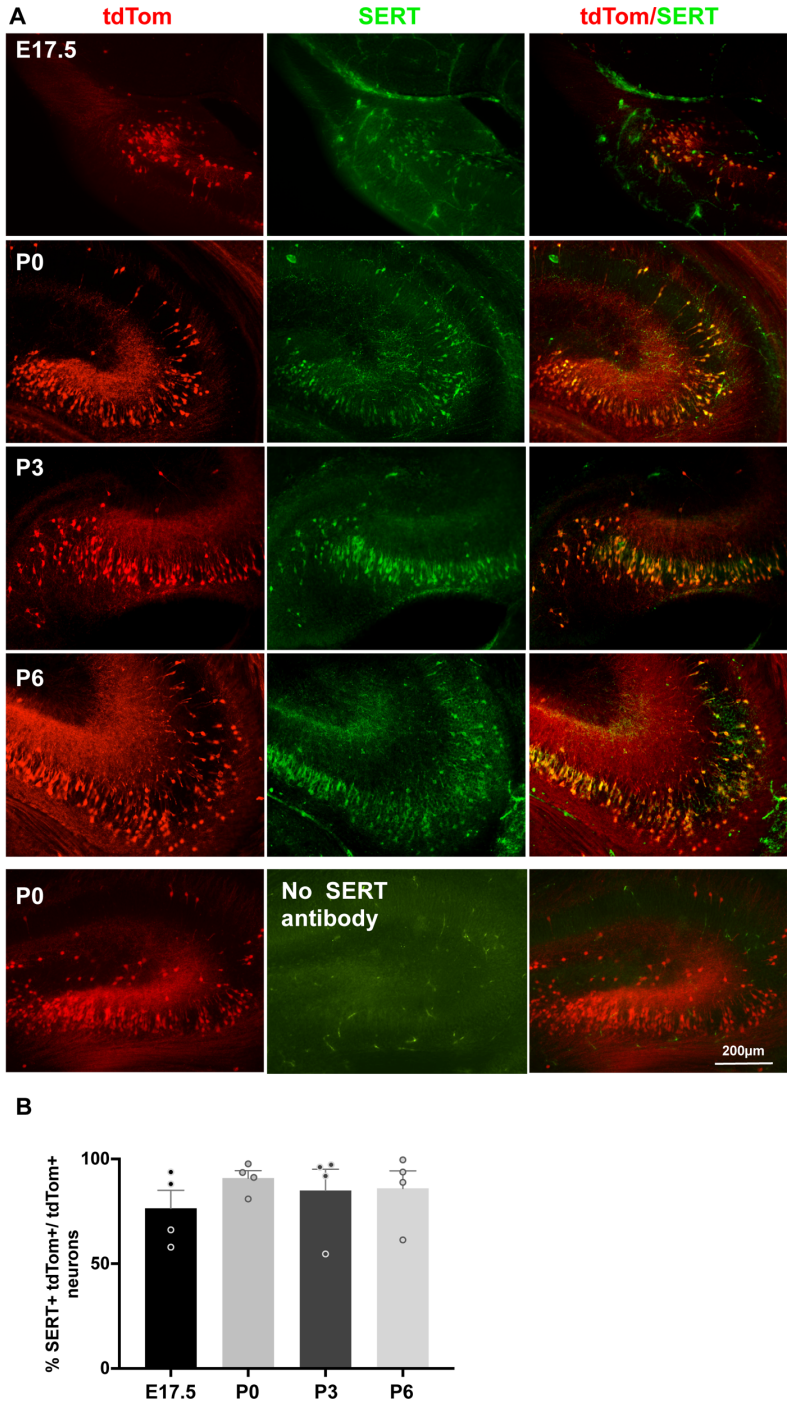

Fig. S2. SERT immunostaining of Cre-dependent tdTomato (tdTom)-expressing neurons in the hippocampus of *SERT*$^{Cre/+}$ mice. **A**. representative images of SERT immunostaining of coronal sections of the hippocampus from *SERT*$^{Cre/+}$ mice at indicated ages. **B.** Quantification of the percentage of tdTom+ neurons displaying detectable SERT immunoreactivity over the total number of tdTom+ neurons located in the CA3 pyramidal layer. n = 4 mice (2 males and 2 females) per age indicated by dots in the bars, mean ± s.e.m. There were no significant differences in the percentage of tdTom+ neurons labeled by SERT immunostaining between the age groups, P = 0.66, one-way ANOVA.

Development • Supplementary information

Fig. S3

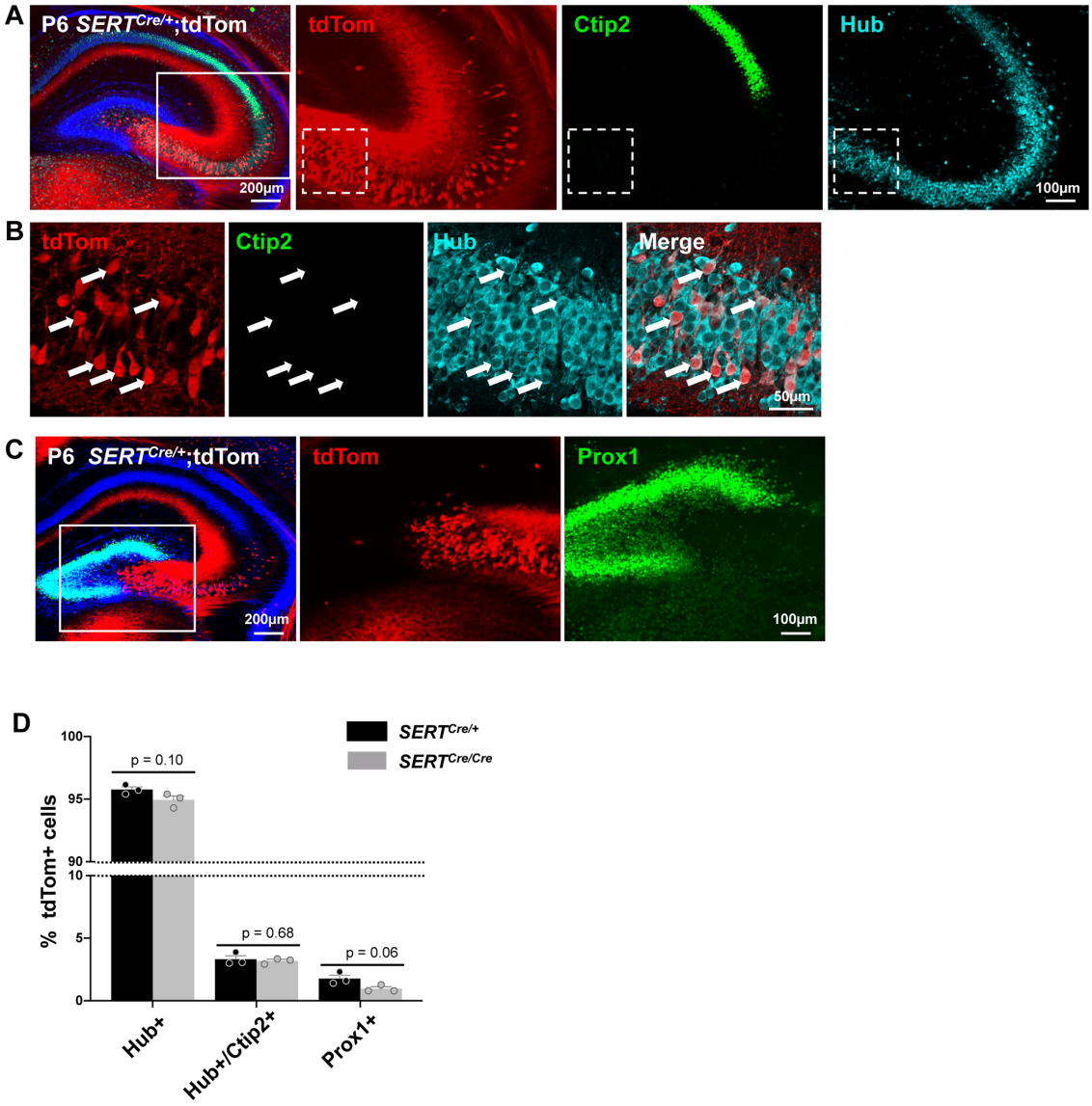

Fig. S3. SERT is not required for cell-fate specification of SERT-expressing CA3 pyramidal neurons. In both *SERT*$^{Cre/Cre}$ (SERT-null)(Soiza-Reilly et al., 2019; Zhuang et al., 2005) and *SERT*$^{Cre/+}$ control mice, SERT-dependent tdTom-expressing neurons displayed robust immunoreactivity to the CA3 pyramidal neuron marker Hub (**A, B**) but not to the CA1 pyramidal neuron marker Ctip2 or the DG granule cell marker Prox1 (**B, C**), with few exceptions (**D**). **A - C** show representative images of double labeling of tdTom and indicated neuronal markers in the hippocampus from *SERT*$^{Cre/+}$ mice. Areas outlined by white solid line boxes are shown in adjacent images of individual staining at a higher magnification, and areas outlined by white dash boxes are shown in confocal images in the **B** panel. Each bar in **D** is mean ± s.e.m. of tdTom-expressing neurons co-labeled with indicated markers in serial coronal sections across the hippocampus. n = 3 mice/genotype, age P6, two-tailed t-test.

Development • Supplementary information

Fig. S4

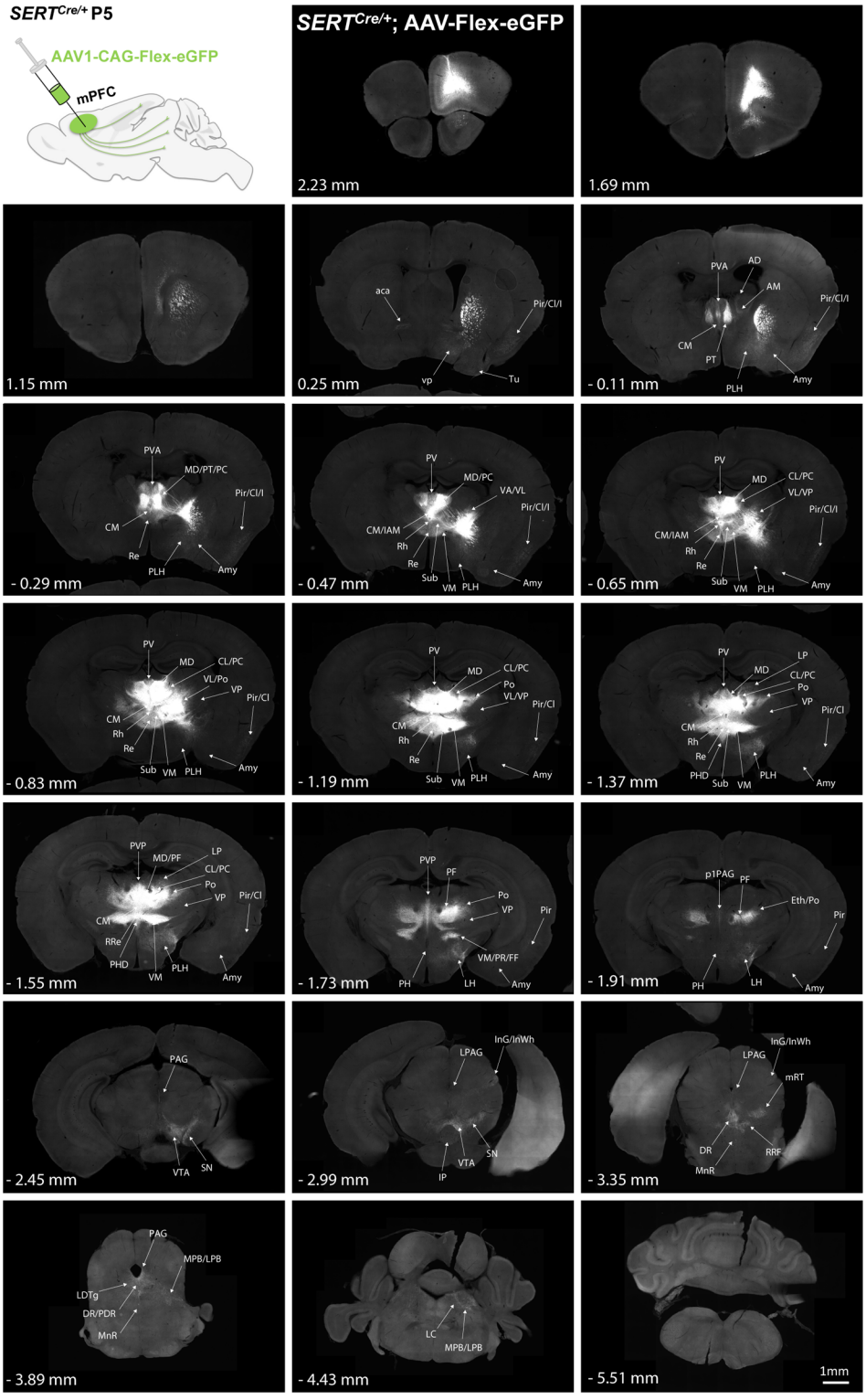

Development • Supplementary information

Fig. S4. Whole brain anterograde tracing of SERT-expressing mPFC pyramidal neuron axonal projections. Top left, a schematics of unilateral stereotaxic injection of AAV1 vector expressing Cre-dependent enhanced GFP (AAV1-CAG-Flex-eGFP) into the mPFC of *SERT*$^{Cre/+}$ mice age P5. **Main** panel shows images of serial sections at indicated distance from the bregma of an injected mouse age P18. GFP was expressed in neurons located at deep layers in the mPFC and their projections targeting to a wide range of cortical and subcortical brain regions, but not to the hippocampus. n = 6 replicates (3 males and 3 females). *aca,* anterior commissure anterior part, and identified target brain region of SERT-expressing mPFC neuron projections are: *AM* anteromedial thalamic nucleus, *Amy* Amigdala, *Cl* Claustrum, *CL* centrolateral thalamic nucleus, *CM* central medial thalamic nucleus, *DR* dorsal raphe nucleus, *Eth* ethmoid thalamic nucleus, *FF* fields of Forel, *I* insular cortex, *IAM* interanteromedial thalamic nucleus, *InG* intermediate gray layer of the superior colliculus, *InWh* intermediate white layer of the superior colliculus, *IP* interpeduncular nucleus, *LC* locus coeruleus, *LH* lateral hypothalamic area, *LP* lateral posterior thalamic nucleus, *LPAG* lateral periaqueductal gray, *LPB* lateral parabrachial nucleus, *LDTg* laterodorsal tegmental nucleus, *MD* mediodorsal thalamic nucleus, *MnR* median raphe nucleus, *MPB* medial parabrachial nucleus, *mRt* mesencephalic reticular formation, *p1PAG* periaqueductal gray, proomer 1, *PAG* periaqueductal gray, *PF* parafascicular thalamic nucleus, *Pir* piriform cortex, *PLH* peduncular part of lateral hypothalamus, *PC* paracentral thalamic nucleus, *PDR* posterodorsal raphe nucleus, *PH* posterior hypothalamic nucleus, *PHD* posterior hypothalamic area, dorsal part, *Po* posterior thalamic nuclear group, *PR* prerubral field, *PT* paratenial thalamic nucleus, *PV* paraventricular thalamic nucleus, *PVA* paraventricular thalamic nucleus, anterior part, *PVP* paraventricular thalamic nucleus, posterior part, *Re* reuniens thalamic nucleus, *RRe* retrouniens area, *RRF* retrorubral field, *Rh* rhomboid thalamic nucleus, *SN* substantia nigra, *Sub* submedius thalamic nucleus, *Tu* Olfactory tubercle, *VA* ventral anterior thalamic nucleus, *VL* ventrolateral thalamic nucleus, *VM* ventromedial thalamic nucleus, *vp* ventral pallidum, *VP* ventral posterior thalamic nucleus, *VTA* ventral tegmental area.

Development • Supplementary information

Figure S5

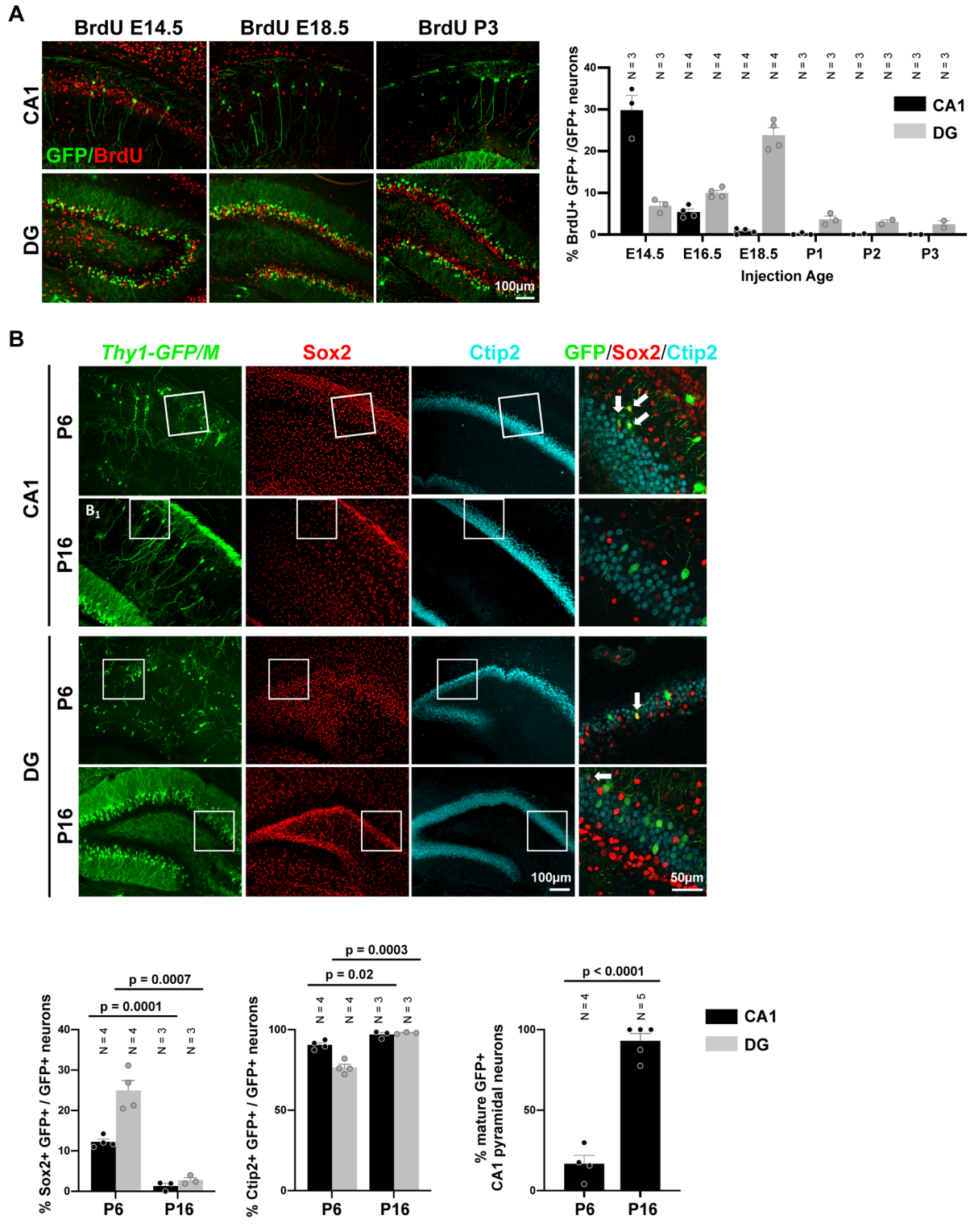

Development • Supplementary information

Fig. S5. Development of *Thy1-GFP/M*-expressing neurons in postnatal hippocampus. **A.** Birth dating *Thy1-GFP/M*-expressing hippocampal neurons using pulse BrdU labeling. *Thy1-GFP/M*-expressing CA1 pyramidal neurons were born prenatally with a peak around E14.5. *Thy1-GFP/M*-expressing DG neurons were born predominantly around E18.5. **Left**, representative images of BrdU and GFP double labelling in CA1 and DG areas of coronal sections of the hippocampus from P16 mice exposed to BrdU at E14.5, E18.5 and P3. **Right**, quantification of the percentage of GFP+ neurons immunolabeled by BrdU over the total number of GFP+ neurons located in CA1 and DG of P16 mice exposed to BrdU at indicated ages. Each dot in the bars represents one mouse, and the number of mice analyzed for each BrdU labeling is indicated on the top of the bars. **B.** Postnatal differentiation of *Thy1-GFP/M*-expressing hippocampal neurons. **Top**, representative images showing co-localization of *Thy1-GFP/M*-expressing CA1 pyramidal neurons and DG granule cells with the immature neuronal marker Sox2 at P6 (indicated by arrows) but rarely at P16. Ctip2 is an established post-mitotic marker for CA1 pyramidal neurons and dentate granule cells. High magnification confocal images of merged staining in areas outlined by white boxes are shown on the right. **Bottom,** left and middle bar graphs show the percentage of *Thy1-GFP/M*-expressing CA1 and DG neurons co-localized with Sox2 and Ctip2, respectively, at P6 and P16. Right bar graph shows the percentage of *Thy1-GFP/M*-expressing CA1 pyramidal neurons displaying mature morphology at P6 and P16, measured based on the presence of 3rd and higher order dendritic branches on the apical dendritic tree. In all the experiments, the number of neurons in serial hippocampal coronal sections was quantified, and the number of mice analyzed is indicated on the top of the bars and represented as dots in the bars, mean ± s.e.m., two-tailed t-test.

Development • Supplementary information

Fig. S6

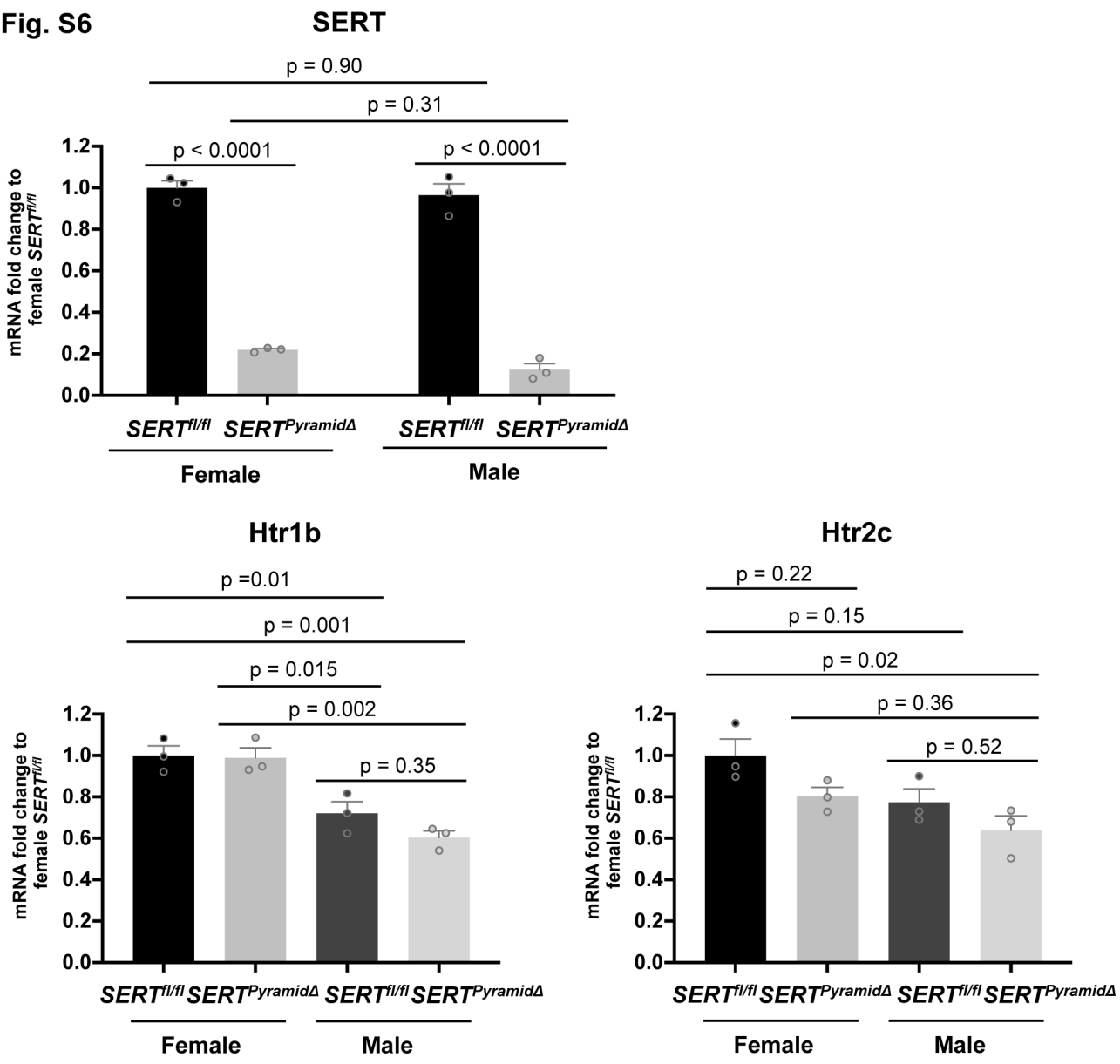

Fig. S6. Expression levels of SERT, 5-HT receptors Htr1b and Htr2c in the hippocampus of males *vs.* females at P7. qPCR analyses of SERT and 5-HT receptor subtypes Htr1b and Htr2c mRNA levels in dorsal hippocampus of P7 $SERT^{PyramidΔ}$ mice and control $SERT^{fl/fl}$ littermates. n = 3 per sex/genotype, each n was pooled dorsal hippocampal tissue from 4 mice. Mean ± s.e.m., two-way ANOVA followed by Tukey post hoc test. SERT: sex effect $F_{1,8}$ = 3.31, P = 0.1060, genotype effect $F_{1,8}$ = 510.6, P<0.0001, interaction $F_{1,8}$ = 0.7149, P = 0.4224. Htr1b: sex effect $F_{1,8}$ = 50.5, P = 0.0001, genotype effect $F_{1,8}$ = 1.89, P=0.2060, interaction $F_{1,8}$ = 1.27, P = 0.2918. Htr2c: sex effect $F_{1,8}$ = 8.80, P = 0.0180, genotype effect $F_{1,8}$ = 6.38, P = 0.0354, interaction $F_{1,8}$ = 0.22, P = 0.6449.

Development • Supplementary information

Table S1. Two-way ANOVA and post hoc analyses of datasets presented in indicated figures.

Click here to download Table S1

Table S2. Differential expression analyses of RNA-seq data comparing male *SERT*$^{fl/fl}$ *vs.* male *SERT*^{PyramidD} hippocampus.

Click here to download Table S2

Table S3. Differential expression analyses of RNA-seq data comparing female *SERT*$^{fl/fl}$ *vs*. female *SERT*^{PyramidD} hippocampus.

Click here to download Table S3

Table S4. GO Terms shown in Figure 6B obtained through DAVID functional annotation analyses of DEGs from RNA-seq defined by P≤0.05.

Click here to download Table S4

Table S5. GO Terms from DAVID functional annotation analyses of DEGs in males from RNA-seq defined by P≤0.01.

Click here to download Table S5

Table S6. GO Terms from DAVID functional annotation analyses of DEGs in females from RNA-seq defined by P≤0.01.

Click here to download Table S6

Development • Supplementary information

Table S7. GO Terms from DAVID functional annotation analyses of DEGs in males from RNA-seq defined by P≤0.005.

Click here to download Table S7

Table S8. GO Terms from DAVID functional annotation analyses of DEGs in females from RNA-seq defined by P≤0.005.

Click here to download Table S8

Table S9. Fisher's exact test for enrichment of cell-type specific gene set (Cahoy et al., 2008) and SFARI gene datasets (gene.sfari.org) within DEGs from RNA Seq defined by P≤0.05, P≤0.01 and P≤0.005.

Click here to download Table S9

Table S10. Qiagen IPA gene enrichment analyses of male DEGs from RNA-seq defined by P≤0.05.

Click here to download Table S10

Table S11. Qiagen IPA gene enrichment analyses of female DEGs from RNA-seq defined by P≤0.05.

Click here to download Table S11

Table S12. Oligo sequences used in qPCR analyses.

Click here to download Table S12

References

Cahoy, J. D., Emery, B., Kaushal, A., Foo, L. C., Zamanian, J. L., Christopherson, K. S., Xing, Y., Lubischer, J. L., Krieg, P. A., Krupenko, S. A., et al. (2008). A transcriptome database for astrocytes, neurons, and oligodendrocytes: a new resource for understanding brain development and function. *J Neurosci* **28**, 264-278.

Soiza-Reilly, M., Meye, F. J., Olusakin, J., Telley, L., Petit, E., Chen, X., Mameli, M., Jabaudon, D., Sze, J. Y. and Gaspar, P. (2019). SSRIs target prefrontal to raphe circuits during development modulating synaptic connectivity and emotional behavior. *Mol Psychiatry* **24**, 726-745.

Zhuang, X., Masson, J., Gingrich, J. A., Rayport, S. and Hen, R. (2005). Targeted gene expression in dopamine and serotonin neurons of the mouse brain. *J Neurosci Methods* **143**, 27-32.

Development • Supplementary information